Aharonov-Bohm phase operations on a double-barrier nanoring charge qubit

Yuquan Wang, Ning Yang, and Jia-Lin Zhu*

Department of Physics, Tsinghua University, Beijing 100084, People's Republic of China
(Received 27 April 2006; published 27 July 2006)

We present a scheme for charge qubit implementation in a double-barrier nanoring. The logical states of the qubit are encoded in the spatial wave functions of the two lowest energy states of the system. The Aharonov-Bohm phase introduced by magnetic flux, instead of tunable tunnelings, along with electric fields can be used for implementing the quantum gate operations. During the operations, the external fields should be switched smoothly enough to avoid the errors caused by the transition to higher-lying states. The structure and field effects on the validity of the qubit are also studied.

I. INTRODUCTION

Solid-state systems seem to be good candidates for quantum computing implementations. In some schemes, qubits can be encoded in nuclear (or electron) spin states.[1,2] Although spin states have relatively long decoherence times (~ms), spin operations are rather slow processes. Besides, the single-spin measurement[3,4] is still a great challenge. Many recent researches focus on charge-based quantum computing technology,[5–7] in which qubits are encoded in the charge degrees of freedom. Charge-based qubits have shorter decoherence times (~ns for GaAs (Ref. [8]) and maybe much longer in some other materials[9]) than their spin-based counterparts. Yet all quantum gates can be done in very short times (~ps), which are well below the decoherence times. The initialization and readout of charge qubits have been proposed.

For charge-qubit implementation, a typical scheme is a coupled quantum dots (CQDs) system with an electron tunneling back and forth.[9] It can be easily scaled up based on the staggered CPHASE or CNOT configuration.[5] Such a scheme, however, is based on the variability of the tunneling.[9–11] In many physical quantum systems, the handle on the tunneling is limited or impossible. Then the implementation of full single-qubit manipulation requires tunable external magnetic fields and the architecture of the system must be elaborately designed.[11,12]

Nowadays, benefiting from new fabrication and experiment techniques, we can fabricate a ringlike quantum dot, namely nanoring, with various materials, such as InAs/GaAs,[13–16] Si,[17,18] SiGe,[19,20] and so on.[21] Its ringlike geometry is suitable for observing the Aharonov-Bohm (AB) effect. It has been shown that additional structures, such as two barriers or impurities can bring unique electronic and transport characters to the system. There are two important modes of AB oscillations in a double-barrier nanoring named X and O modes.[22] The ground state entanglement with environment[23,24] and the persistent current oscillations[24,25] are also widely studied. To a certain extent, such a system can be viewed as CQDs with a multiply connected domain. Then it may serve as a charge qubit and facilitate the quantum operation by changing the AB phase caused by the magnetic flux.

Employing the external fields to modify the wave functions of an electron in nanostructures is the foundation of solid quantum computation. So in this work, we will study the evolutions of the wave functions and demonstrate the validity of the charge qubit based on the double-barrier nanoring. Full single-qubit operations can be carried out by electric fields and magnetic flux. The remainder of this paper is organized as follows. The descriptions of model Hamiltonian and the calculation method for the evolution of states are presented in Sec. II. Main results and discussions are given in Sec. III followed by a summary in Sec. IV.

II. MODEL SYSTEM

The model Hamiltonian for an electron in a two-dimensional ring with two identically sectorial barriers, subjected to a magnetic flux ϕ and an in-plane electric field F applied along the axis $\theta=0$, as shown in Fig. 1, is written as

$$H = \left(-i\,\nabla + \frac{\phi}{|\mathbf{r}|}\right)^2 + V_c + V_g + \mathbf{F} \cdot \mathbf{r}, \tag{1}$$

where r_a and r_b are, respectively, the inner and outer radii. V_c is the hard wall potential which is 0 in the ring and infinite elsewhere. V_g are the barriers in the ring whose height are V_0 in the barriers and 0 elsewhere. The width of the barrier is selected quite small to ensure that the wave function has maximally one angular node inside each barrier. Here we use the effective atomic units, in which the effective Rydberg $\mathrm{Ry}^* = m_e^* e^4/2\hbar^2\ (4\pi\varepsilon_0\varepsilon_r)^2$, the effective Bohr radius $a_B^* = 4\pi\varepsilon_0\varepsilon_r\hbar^2/m_e^* e^2$, and $\phi_0 = 2\pi\hbar c/e$ are taken to be the energy, length, and magnetic flux units, respectively. The units
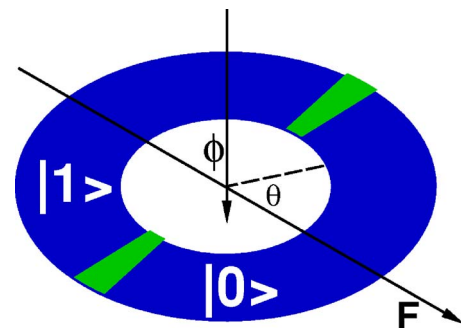

FIG. 1. (Color online) Scheme of a parallel double-barrier nanoring subject to a magnetic flux and an in-plane electric field.

for the electric field is $F_0 = \text{Ry}^*/ea_B^*$. For InAs/GaAs materials, for example, $\text{Ry}^* = 5.8$ meV, $a_B^* = 10$ nm, and $F_0 = 5.8$ kV/cm. ϕ_0 included by a one-dimensional (1D) ring with a radius of 10 nm corresponds to the magnetic field 13.18 T.

The eigenenergies E_n and corresponding eigenstates ψ_n of the double-barrier nanoring were computed by direct diagonalization of the Hamiltonian in a basis set of 59 eigenstates of the same nanoring without a barrier.[22] Since the nanoring is divided into two segments by the barriers, the electron states localized in right and left segments can be, respectively, regarded as the logical state $|0\rangle$ and $|1\rangle$, as will be shown below.

In order to demonstrate the implementation of quantum gate operations, we need to calculate the evolutions of the states when **F** and ϕ are changing. Assume that the Hamiltonian is the sum of H and $H'(t)$, where $H'(t)$ is the change of the Hamiltonian from time $t = 0$, the time evolution of a state

$$\psi(t) = \sum_k C_k(t) \exp\left(-\frac{i}{\hbar} E_k t\right) \psi_k \tag{2}$$

is given by

$$i\hbar \frac{dC_n(t)}{dt} = \sum_k C_k(t) \langle \psi_n | H'(t) | \psi_k \rangle \exp\left[\frac{i}{\hbar}(E_n - E_k)t\right].$$

This ordinary differential equation set was solved by the Runge-Kutta method. Then we could explore the external field and structure effects in implementations of different gate operations.

III. ANALYSIS

For the nanoring with a hard-wall potential, we can, respectively, define the radius R and the width W as the average value of inner and outer radii and the difference between them.

A. Energy spectra and qubit definition

In our scheme of charge qubit, the logical states are encoded in the wave functions of the first two states of the double-barrier nanoring. Due to the AB effect, it can be seen from the energy spectra in Fig. 2(a) that the ground state (ψ_1) and first excited state (ψ_2) of a parallel double-barrier nanoring (the angle between two barriers is equal to π) are degenerate when $\phi = 0.5\phi_0$ and **F** $= 0$. These two occasionally degenerate states are just X-type states which had been discussed in a previous work.[22] The virtue of this condition is that the qubit can be frozen in any linear superposition in its qubit space to avoid unnecessary evolutions in idle time. This request can also be satisfied by applying high enough barriers, just like the situation in a CQDs system. It is convenient to take the normalized sum and difference of the two states $(\psi_1 \pm \psi_2)/\sqrt{2}$ as logical states $|0\rangle$ and $|1\rangle$, respectively. Within such a choice, the electron of state $|0\rangle$ ($|1\rangle$) is almost completely localized in the right (left) segment of the ring. The energy spectra for a nonparallel double-barrier nanoring
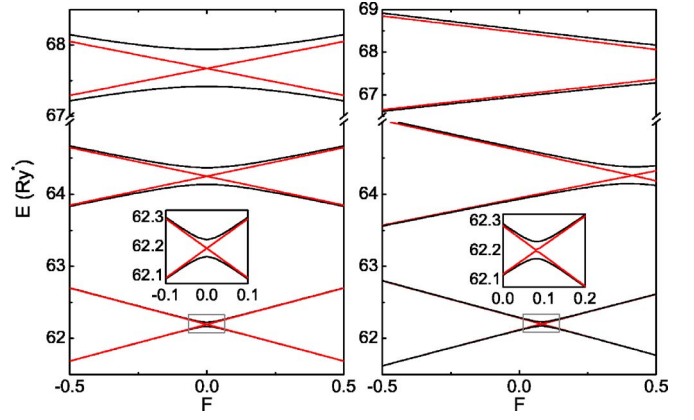

FIG. 2. (Color online) **F**-dependence of energy spectra of the nanoring with two parallel barriers (a) and nonparallel barriers (b) with $R = 1.2a_B^*$, $W = 0.4a_B^*$, $V_0 = 90$ Ry*, $\phi = 0$ (black lines) and $0.5\phi_0$ (red lines), respectively. The first two levels are also shown in the inset for clarity.

are shown in Fig. 2(b). The first two energy levels can still be tuned to degenerate by **F** with $\phi = 0.5\phi_0$. So the qubit states can always be defined properly to avoid needless evolutions. Due to the inherent ringlike geometry of the system, in our charge qubit scheme it is much easier to implement AB phase operation than that in CQDs. In the remainder of the paper, we will focus on a parallel double-barrier nanoring with an initial magnetic flux $\phi = 0.5\phi_0$. The initialization of qubit states to the state $|0\rangle$ can be realized by applying an appropriate electric field along the axis $\theta = 0$. The readout can be implemented by a single-electron transistor[26] (SET) or quantum point contact[27–29] (QPC) detector. Because the double-barrier nanoring can also be viewed as a new kind of CQDs, the qubit based on it can be scaled up by a present CPHASE configuration scheme.[5]

B. State evolutions with F and ϕ

With logical states $|0\rangle$ and $|1\rangle$ defined, we can calculate the evolutions of the wave functions and qubit states with the change of external parameters by employing the Runge-Kutta method. We will present the results concentrating on the characters of evolutions in this subsection. The quantitative analyses are left to the next subsection.

From Hamiltonian (1) it can be imagined that changing the magnetic flux, the height of the two barriers and the electric field all can achieve some evolutions of wave functions. In Figs. 3(a) and 3(b) we illustrate the evolutions of wave functions when applying an in-plane electric field along $\theta = 0$ from $t = 0$. The positions of the barriers are indicated by the vertical dashed lines. The initial states are both ψ_1, although the wave functions are not the same because V_g is infinite and $\phi = 0$ in Fig. 3(a) but $\phi = 0.5\phi_0$ and V_g is finite in Fig. 3(b). Both conditions make the states ψ_1 and ψ_2 degenerate. After some time the final states can be both ψ_2, although their wave functions are not equal either. Recalling the definition of logical states of the qubit, the initial and final states are just $(|0\rangle + |1\rangle)/\sqrt{2}$ and $(|0\rangle - |1\rangle)/\sqrt{2}$, respectively. It can be seen from the third row of Figs. 3(a) and 3(b)
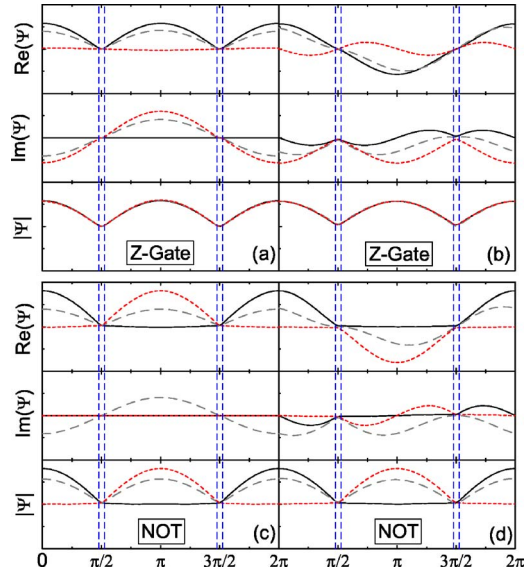
FIG. 3. (Color online) The evolutions of wave functions during the Z-gate operations by applying **F** with $V_0 \to \infty$ and $\phi = 0$ (a) or finite V_0 and $\phi = 0.5\phi_0$ (b), the NOT-gate operations by changing V_0 with $\phi = 0$ (c) or changing ϕ with fixed finite V_0 (d). The real and imaginary parts and the modulus of the wave functions are plotted in three rows, respectively. Different line styles represent the quantities at different times. The black solid lines and red dotted lines represent the quantities at the starting and ending time, respevtively. The vertical dashed lines indicate the positions of the two barriers.
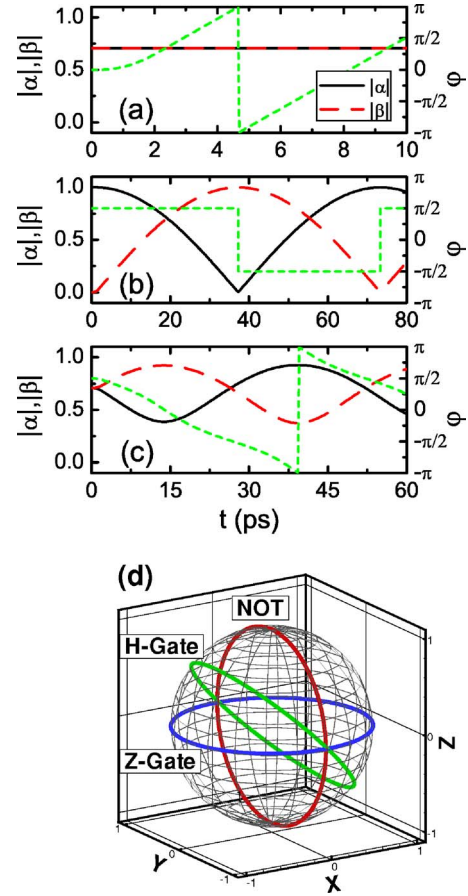

FIG. 4. (Color online) Evolutions of the qubit states with in-plane electric field pulse (a), magnetic flux pulse (b), and both fields together (c). Black solid, red dashed, and green dotted lines correspond to the square root of probability density of the state occupying $|0\rangle$, $|1\rangle$, and the phase difference, respectively. The trajectories of Bloch vectors corresponding with the evolutions in (a)–(c) are shown in (d) noted as Z, NOT, and H gate, respectively.

that the moduli of the wave functions are unchanged during the evolutions. This evolution is just the single-qubit gate operation, namely the Z gate, which will be discussed in the following section.

One goal of the paper is to identify the similar effects of changing the AB phase and the barrier heights on the qubit operations. Thus we verify the evolutions of wave functions when changing the barrier heights and the magnetic flux from $t = 0$. The results are shown in Figs. 3(c) and 3(d). The initial states are both logical state $|0\rangle$ with different wave functions, because there is no flux in Fig. 3(a) but $0.5\phi_0$ flux before $t = 0$ in Fig. 3(b). It can be found that the final states are both $|1\rangle$. It means that the two methods can implement similar quantum operations on the logical states of the qubit. From Fig. 2 it can be seen that the crossing of the first two states becomes anticrossing when $\phi \neq 0.5\phi_0$, which means that the two states can mix up. Similar with varying the barrier height, the change of the flux determines the admixture level. So in the following, we will adopt the magnetic flux, instead of the barrier height, and the electric field to explore the evolutions of the qubit states.

The first case with which we are concerned is still the electric field. An in-plane electric field applied along the axis $\theta = 0$ from $t = 0$ makes the energies of one electron localized in the left and right segments unequal. As shown in Fig. 3(b) and Fig. 4(a), the electric field will not change the probability of the states projecting to $|0\rangle$ or $|1\rangle$. It can only bring a phase difference between the two components. The trajectory of Bloch vector corresponding to such an evolution is a rotation around the z axis of the Bloch sphere.

The situation is different when the magnetic flux changes. Because we have assumed that there is an always-on magnetic flux $\phi = 0.5\phi_0$, we will decrease this flux from $t = 0$ and the initial state is chosen to be $|0\rangle$ without electric fields. Then the degeneracy of $|0\rangle$ and $|1\rangle$ is removed, and the mixture of the two states forms a cycle trajectory of the Bloch vector around the x axis of Bloch sphere. From Fig. 4(b) we can see that the variation of the flux changes the probability of each component. It also changes the sign of the phase difference when the Bloch vector rotates half a cycle.

By applying both the electric field and magnetic flux pulse, we can implement arbitrary rotation of the Bloch vector. In Fig. 4(c), we plot one of such rotations, which can be used for implementing the Hadamard gate.

C. Characters of quantum operations

Through the above analysis, it is straightforward to implement the single-qubit quantum operations by applying the electric field and changing the magnetic flux.

The first important gate operation is the Z gate which implements the transform from $\alpha|0\rangle + \beta|1\rangle$ to $\alpha|0\rangle - \beta|1\rangle$,
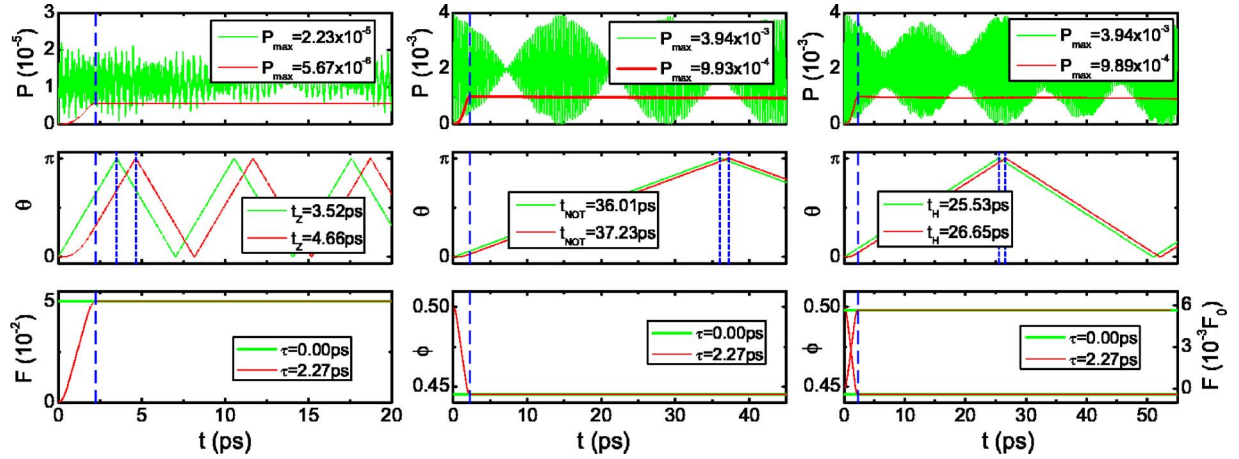
FIG. 5. (Color online) Control parameter settings (the bottom row), angular evolutions (the middle row) of Bloch vectors in the plane of their trajectories, and probabilities (the upper row) lost from the qubit space to higher states under the operation of the Z (left column), NOT (middle column), and Hadamard gate (right column). The size of the ring is $R=1.2a_B^*$, $W=0.4a_B^*$, and $V_0=90$ Ry*. The red and green lines correspond to different pulsing forms.

where α and β are arbitrary constants. Applying an electric field and controlling the pulse duration to make the angle of rotation equal to π just achieves a Z-gate operation. As shown in the left column of Fig. 5, for the nanoring subjected to a magnetic flux $\phi=0.5\phi_0$ with $R=1.2a_B^*$, $W=0.4a_B^*$, and $V_0=90$ Ry*, the time for completing a Z-gate operation is 4.66 ps if the amplitude of the electric pulse is $0.05F_0$. This operation time is much smaller than the typical charge decoherence time for GaAs.

In order to implement full single-qubit operations, we still need an operation which can make the Bloch vector rotate around another axis other than the z axis. This operation can be achieved by changing the magnetic flux[11] as discussed in the previous subsection. In the middle column of Fig. 5, we have shown such an operation by changing the flux from $0.5\phi_0$ to $0.445\phi_0$ from $t=0$. The electric field is set to zero. When the rotation angle of the Bloch vector is again equal to π, we can get the NOT-gate which changes the state $|0\rangle$ to $|1\rangle$ and vice versa. The time for the NOT operation is 37.23 ps, which is a little longer than the Z-gate but still much smaller than the decoherence time.

With these two operations, we can implement arbitrary single-qubit operations. For example, the Hadamard gate, which may be the most important single-qubit gate in quantum computation, can be achieved by accurately controlling the external fields and the operation time as shown in the right column of Fig. 5. With the pulses $\mathbf{F}=0.005\,63F_0$ and $\phi=0.445\phi_0$, the time for a Hadamard operation is 26.65 ps.

Besides the operation time, there is still another important index of quantum gate. We know that there is a small fraction of probability (P) which is lost from the first two states to the higher-lying ones during every gate operation. This phenomenon will result in errors in quantum computation and may also be considered as a decoherence source. Then this probability must be regarded as an important judgment of the validity of the qubit scheme.

In Fig. 5 we have shown two kinds of probability loss corresponding to different forms of the external field pulses. It can be seen that the value of P can be less than 0.1% if the

pulse has a smooth rising or trailing edge. Although such an error rate is still greater than the threshold (10^{-4} for an estimated value widely accepted at present) for fault-tolerance quantum computation, it is indeed small enough for coherence quantum operations in single-qubit experiments. If the changes of external field parameters are instantaneous, P will be much larger and have severe vibration for both electric fields and magnetic flux. This also coincides with the idea that the evolution of the qubit states should be adiabatic during the quantum operations. A smooth change of the fields ensures such a premise.

D. Structure and field effects

In this section, we will discuss the structure and field effects on the validity of our qubit and corresponding operations.

First of all, we have chosen the two localized states of the electron in a double-barrier nanoring as the logical states $|0\rangle$ and $|1\rangle$. However, because of the finite height of the two barriers, these two states are not completely localized in one segment of the ring. The state mainly localized in one segment indeed has a probability (Δ) expanding to another segment. This probability leads to errors in readout process and must be limited to a tiny value. It can be seen from Fig. 6(a) that the probability can be depressed by choosing appropriate V_0 for different R. And the larger R is, the lower V_0 is needed.

Second, we have seen that changing the magnetic flux can implement the NOT-gate operation. But its operation time is longer than the Z gate which is implemented by applying a small electric field. Of course, this operation time is related to the amplitude of the change of the flux. It can be seen in Fig. 6(b) that increasing the change of the flux can apparently speed the operation. But on the other hand, it also increases the probability loss during the operation. So in our calculation, we have chosen the field parameters carefully, to ensure both a short operation time and a small P. It is worthwhile to note that the value of V_0 can also affect the opera-
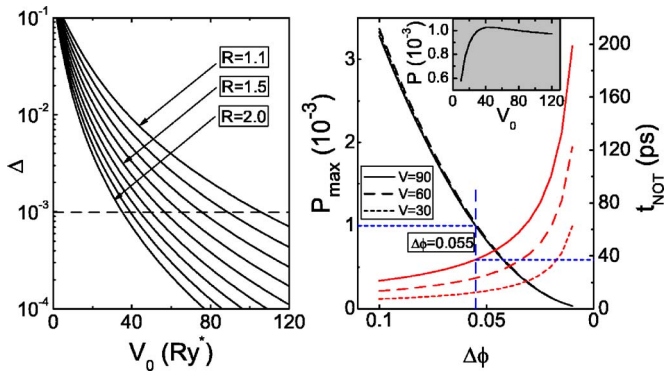
FIG. 6. (Color online) (a) Error probability (Δ) as functions of V_0 with different R. The curves correspond to $R=1.1a_B^*$ to $R=2.0a_B^*$ from the top down. (b) Maximal probability loss (P_{max}) and operation time (t_{NOT}) as functions of the change of magnetic flux ($\Delta\phi$) with three different V_0 (plotted with different line styles) during the NOT-gate operation. The V_0 dependence of P is shown in the inset. In all the cases, $W=0.4a_B^*$.

FIG. 7. (Color online) Operation time for the NOT gate as a function of R and V_0. An example of appropriate choice of the structural parameters is illustrated by the green line and its projection to the R-t_{NOT} plane is plotted in the inset.

tion time and P. Lower barriers can speed the operation and decrease P. But in fact, it must be selected high enough to avoid the increase of Δ.

Finally, we present R and V_0 dependence of the operation time for the NOT gate in Fig. 7. It can be found intuitively that large radius R and high barriers V_0 will dramatically increase the operation time. An appropriate choice of the structural parameters is illustrated by the green line in Fig. 7 where small rings correspond to high barriers and large rings correspond to low barriers. Such selections can take into account both the speed of the operation and tolerable errors.

IV. SUMMARY

A scheme of qubit based on one electron's charge degree of freedom in a double-barrier nanoring is presented. Because the first two states of the system are degenerate when $\phi=0.5\phi_0$, the logical states can be frozen in any linear superposition in the qubit space to avoid unnecessary evolu-
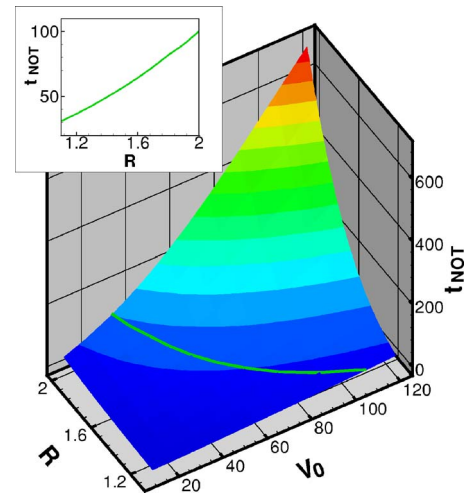
tions. The electric fields can implement the z-axis gate operations of the qubit. By virtue of the ringlike geometry of the system, the x-axis operations can be achieved by the AB effect of the magnetic flux. As a result, full qubit operations can be implemented even if the barrier height is kept constant. The structure and field effects are important for the validity of the qubit. The external field pulse should also have an appropriate rising or trailing edge to decrease the transition of the electron to higher-lying states. The radius and barrier height should be selected appropriately to speed the operations and depress the errors. These results will be helpful in understanding the evolutions of wave functions during the quantum operations and useful for the future implementation of qubits in a solid system.

*Email address: zjl-dmp@tsinghua.edu.cn

[1] B. E. Kane, Nature (London) **393**, 133 (1998).

[2] V. N. Golovach and D. Loss, Semicond. Sci. Technol. **17**, 355 (2002).

[3] J. M. Elzerman, R. Hanson, L. H. W. van Beveren, B. Witkamp, L. M. K. Vandersypen, and L. P. Kouwenhoven, Nature (London) **430**, 431 (2004).

[4] A. D. Greentree, A. R. Hamilton, L. C. L. Hollenberg, and R. G. Clark, Phys. Rev. B **71**, 113310 (2005).

[5] L. C. L. Hollenberg, A. S. Dzurak, C. Wellard, A. R. Hamilton, D. J. Reilly, G. J. Milburn, and R. G. Clark, Phys. Rev. B **69**, 113301 (2004).

[6] L. A. Openov, Phys. Rev. B **70**, 233313 (2004).

[7] S. D. Barrett and T. M. Stace, Phys. Rev. Lett. **96**, 017405 (2006).

[8] T. Hayashi, T. Fujisawa, H. D. Cheong, Y. H. Jeong, and Y. Hirayama, Phys. Rev. Lett. **91**, 226804 (2003).

[9] J. Gorman, E. G. Emiroglu, D. G. Hasko, and D. A. Williams, Phys. Rev. Lett. **95**, 090502 (2005).

[10] L. Fedichkin, M. Yanchenko, and K. A. Valiev, Nanotechnology **11**, 387 (2000).

[11] A. Weichselbaum and S. E. Ulloa, Phys. Rev. A **70**, 032328 (2004).

[12] A. Weichselbaum and S. E. Ulloa, Phys. Rev. B **70**, 195332 (2004).

[13] A. Lorke, R. J. Luyken, A. O. Govorov, J. P. Kotthaus, J. M. Garcia, and P. M. Petroff, Phys. Rev. Lett. **84**, 2223 (2000).

[14] A. Fuhrer, S. Lüscher, T. Ihn, T. Heinzel, K. Ensslin, W. Wegscheider, and M. Bichler, Nature (London) **413**, 822 (2001).

[15] U. F. Keyser, S. Borck, R. J. Haug, M. Bichler, G. Abstreiter, and

W. Wegscheider, Semicond. Sci. Technol. **17**, L22 (2002).

[16] D. Granados and J. M. García, Appl. Phys. Lett. **82**, 2401 (2003).

[17] K. L. Hobbs, P. R. Larson, G. D. Lian, J. C. Keay, and M. B. Johnson, Nano Lett. **4**, 167 (2004).

[18] J. H. He, W. W. Wu, Y. L. Chueh, C. L. Hsin, L. J. Chen, and L. J. Chou, Appl. Phys. Lett. **87**, 223102 (2005).

[19] N. Jiang, G. G. Hembree, J. C. H. Spence, J. Qiu, F. J. Garcia de Abajo, and J. Silcox, Appl. Phys. Lett. **83**, 551 (2003).

[20] J. H. He, Y. L. Chueh, W. W. Wu, S. W. Lee, L. J. Chen, and L. J. Chou, Thin Solid Films **469**, 478 (2004).

[21] X. Y Kong, Y. Ding, R. Yang, and Z. L. Wang, Science **303**, 1348 (2004).

[22] J.-L. Zhu, X. Q. Yu, Z. H. Dai, and X. Hu, Phys. Rev. B **67**, 075404 (2003).

[23] P. Cedraschi and M. Bütiker, Ann. Phys. **289**, 1 (2001).

[24] M. Büttiker and A. N. Jordan, Physica E (Amsterdam) **29**, 272 (2005).

[25] M. Büttiker and C. A. Stafford, Phys. Rev. Lett. **76**, 495 (1996).

[26] A. Aassime, G. Johansson, G. Wendin, R. J. Schoelkopf, and P. Delsing, Phys. Rev. Lett. **86**, 3376 (2001).

[27] E. Buks, R. Schuster, M. Heiblum, D. Mahalu, and V. Umansky, Nature (London) **391**, 871 (1998).

[28] S. Pilgram and M. Büttiker, Phys. Rev. Lett. **89**, 200401 (2002).

[29] S. A. Gurvitz, L. Fedichkin, D. Mozyrsky, and G. P. Berman, Phys. Rev. Lett. **91**, 066801 (2003).